CHAPTER 5

Hydrogen Sensing Properties of Colloidal ZnO Quantum Dots Thin Film Based Interdigitated MSM Device*

Contents

*Part of this work has been published as:

1. **Smrity Ratan,** Chandan Kumar, Amit Kumar, Deepak Kumar Jarwal, Ashwini Kumar Mishra, Rishibrind Kumar Upadhyay, and Satyabrata Jit, "Fabrication and characterization of a ZnO quantum dots-based metal-semiconductor-metal sensor for hydrogen gas," ***Nanotechnology***, vol. 30, no. 39, pp. 7, 2019.

CHAPTER 5

Hydrogen Sensing Properties of Colloidal ZnO Quantum Dots Thin Film Based Interdigitated MSM Device

5.1 Introduction

After observing the non-suitability of the sol-gel derived TiO_2 thin films for room-temperature hydrogen sensing in Chapter-2, Chapter-3 and Chapter-4 have been devoted the hydrogen sensing properties of the thermally evaporated and electron beam evaporated TiO_2 thin films respectively. The literature survey carried out in Chapter-1 shows that ZnO thin films have good hydrogen gas sensing properties [Zhang *et al.* (2010), Forleo *et al.* (2010), Ra *et al.* (2010), Ranwa *et al.* (2016)]. However, significant work is reported on the hydrogen sensing properties of ZnO quantum dots. It may be mentioned that quantum dots have the highest surface-to-volume ratio among various nanostructures which makes them suitable for gas sensing applications [Luo *et al.* (2017)]. This chapter is thus devoted to investigating the hydrogen sensing properties of the colloidal ZnO quantum dots (QDs) based metal-semiconductor-metal (MSM) structure considered in Chapter-2. To the best of our knowledge, a colloidal ZnO QDs based interdigitated MSM structure has been explored for the H_2 gas sensing for the first time in this work. The ZnO QDs are synthesized by the low-cost solution-processed hot injection method [Y. Kumar *et al.* (2017 *Lett.*)]. The device is shown to operate at relatively lower operating temperatures than other reported H_2 sensors. The outline of the remaining chapter is given below.

Section 5.2 includes the detail of the experimental methodology for the fabrication of ZnO QDs based MSM sensor for hydrogen detection. The electrical and optical

properties of the ZnO QDs based MSM sensor are presented in section 5.3. Finally, section 5.4 includes the summary and conclusion of this chapter.

5.2 Experimental Details

5.2.1 Synthesis of ZnO QDs

Colloidal ZnO QDs are synthesis using solution route from zinc acetate dehydrate. Equal molar of zinc acetate dehydrate (Precursor) with an equal molar of monoethylamine (MEA) (Regent) and 2-methoxyethanol (Coordinating ligand) are used for the synthesis of ZnO QDs as reported by Y. Kumar *et al.* (2017 *Lett.*). First, 200 mM zinc acetate is dissolved in 2-methoxyethanol, and then the solution is stirred continuously in the flow of N_2 gas at room temperature. The temperature of the solution is gradually increased and maintained at 60°C, at which MEA of the equivalent molar ratio is quickly injected into the solution. When the reagent is decomposed completely, the heating of the solution is immediately stopped, and it is brought to normal room temperature. The resultant solution is stirred for 24 hrs in the flow of N_2, which is then filtered using PVDF membrane (0.22 μm). The Transmission Electron Microscopy (TEM) (TECHNAI G2 20 TWIN) study confirms the synthesis of ZnO QD with a particle size of ~2.53 nm, which is smaller than the Bohr's radius (~2.87 nm for ZnO) as reported in [Y. Kumar *et al.* (2017 *Lett.*), Y. Kumar *et al.* (2017 *Trans.*)]. A flow chart for the synthesis of ZnO QDs is shown in Figure 5.1, and synthesized ZnO QDs in a cultural bottle under UV light is shown in Figure 5.2.

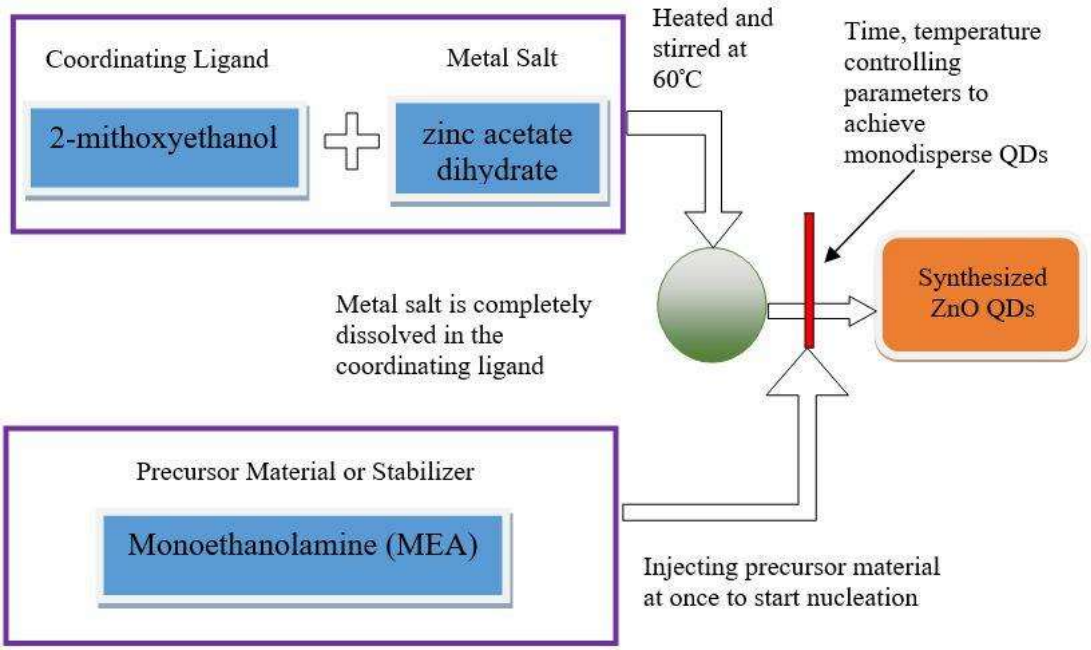

Figure 5.1: Flowchart of ZnO QD synthesis under the inert environment.

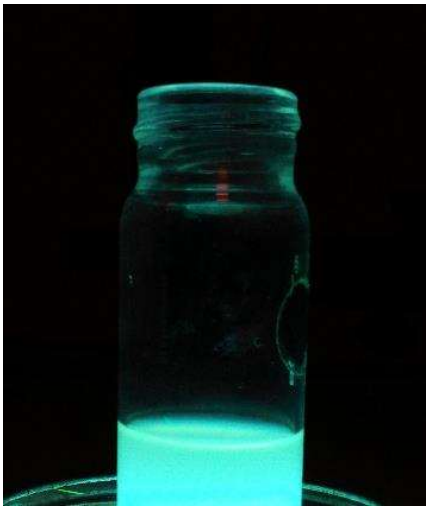

Figure 5.2: Synthesized ZnO QDs.

5.2.2 Thin Film Deposition and Device Fabrication

For the device fabrication, p-type <100> silicon substrates (of 15×15 mm^2 size) with 2-7 Ω.cm resistivity are cleaned according to the method discussed in Chapter 2. The cleaned Si substrates for then processed for dry oxidation in a cylindrical furnace for a thermally grown silicon dioxide (SiO_2) layer of ~300 nm on the substrates. The SiO_2

layer coated Si substrates are then placed on the spin coating (SPM-150LC, GmbH) unit for depositing colloidal ZnO QDs at 3000 rpm for 30 s using 200 mM ZnO QDs solution prepared by the hot-injection method described earlier. The deposited film is dried at 200°C for 10 minutes. The process is repeated 4 times to obtain a total ZnO QDs layer thickness of ~60 nm. Finally, the film is annealed at 450°C on a hot plate for 30 minutes under ambient air conditions. Then the interdigitated MSM electrode pattern with a channel length of 300 μm is obtained (with ~50 nm thickness) on the ZnO QDs thin film using the shadow masking technique. The MSM structure is preferable due to easy fabrication and characterization as well as enhanced sensitivity [Y. Kumar *et al.* (2017 *Lett.*), C. Kumar *et al.* (2018)]. Pure Ag (99.99%) is deposited for forming the electrode structure by a thermal evaporation method (Model No. FL400, Hind HiVac) at a vacuum of ~2×10^{-6} mbar and a deposition rate of ~0.5 nm/s. Finally, the fabricated device is annealed at 400°C using the annealing furnace for 7 minutes in an N_2 atmosphere. The cross-sectional diagram of the as-fabricated sensor is shown in Figure 5.3.

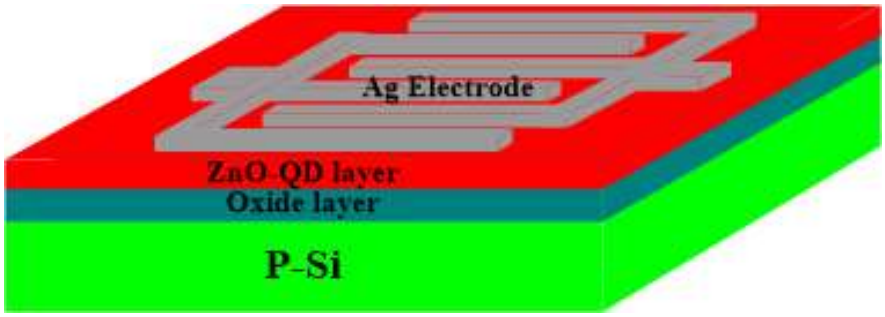

Figure 5.3: The cross-sectional device structure of as-fabricated ZnO QDs based MSM sensor.

5.3 Results and Discussion

In this section, the results of thin-film and electrical as well as gas sensing characterization of MSM sensor are presented.

5.3.1 Thin Film Characterization

Figure 5.4 shows the X-ray diffraction (XRD, Model no. XDMAX, PC-20 18kW Cu rotating anode, RIGAKU) of the ZnO QDs layer on SiO_2/p-Si substrate under investigation. The phase and crystalline structure of the ZnO QDs layer using Cu Kα-radiation (λ = 0.1542 nm) with the XRD angle (2θ) varying from 20° to 60° have been investigated in Figure 5.4. The analysis of the XRD using JCPDS No. 36-1451 shows that the ZnO QDs grown on the SiO_2/Si substrates possess the hexagonal structure with a strong diffraction peak at 33.9° corresponding to (002) facet and others weak peaks at 31.2°, 35.8°, 47.1°, and 56.1° corresponding to the diffractions from the (100), (101), (102) and (110) facets, respectively. These peaks indicate that ZnO QDs are of high quality and phase purity. The peak at 32.3° (200) is due to diffraction from the underneath silicon substrate in the MSM structure.

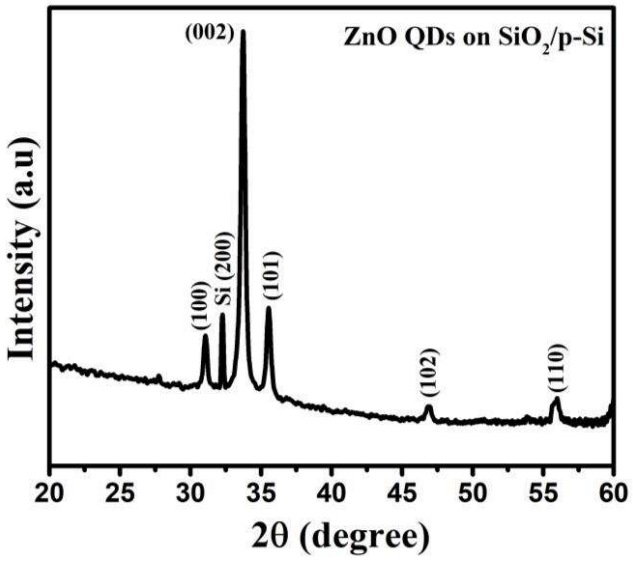

Figure 5.4: XRD image of the ZnO QDs thin film on SiO_2/p-Si substrate.

The result of Energy Dispersive X-Ray Spectroscopy (EDS, from Oxford, UK) of the ZnO QDs deposited on SiO_2/Si substrates is shown in Figure 5.5. It confirms the elemental compositions of zinc, silicon, and oxygen. Smaller peaks of zinc and oxygen than Si are due to the thinner layer of ZnO QDs than the SiO_2/Si substrate thickness.

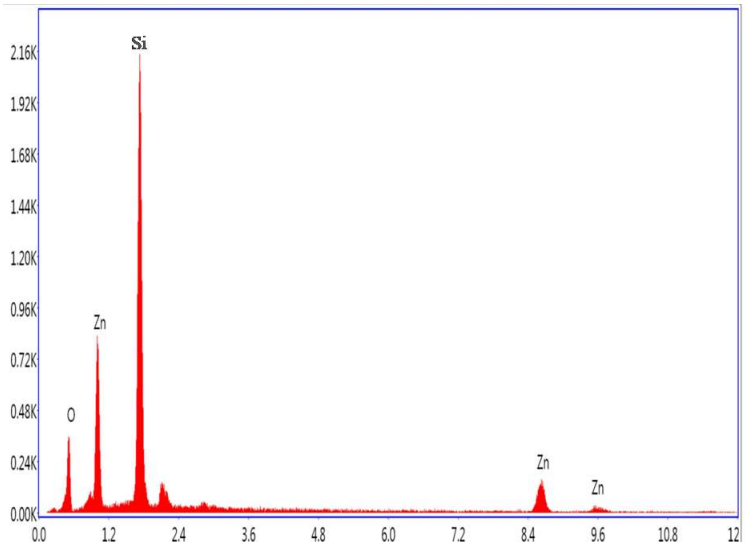

Figure 5.5: EDS image of ZnO QDs deposited on the silicon substrate.

Scanning electron microscopy (SEM, Model: EVO MA 15/18, from Carl Zeiss Microscopy Ltd., UK) measurement of the as-fabricated device after annealing at 450°C is obtained and shown in Figure 5.6.

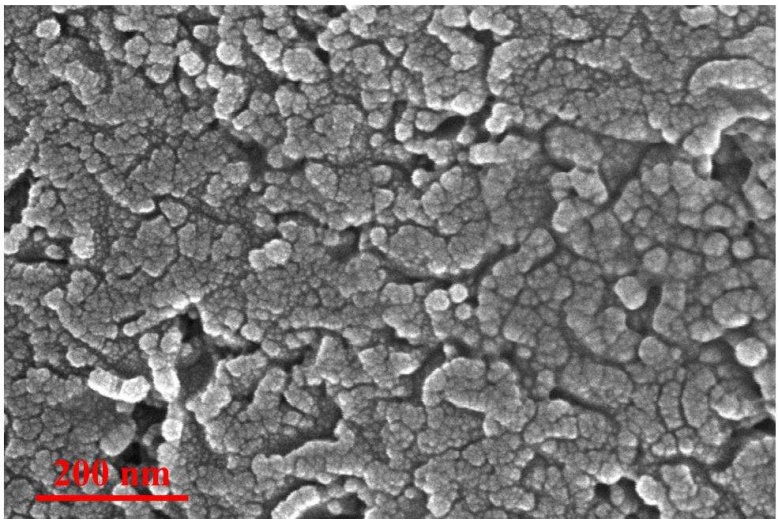

Figure 5.6: SEM image of ZnO QDs thin film on Si/SiO_2 substrate annealed at 450°C.

As compared to the particle size of as-grown ZnO QDs (i.e. 2.53 nm) [Y. Kumar *et al*. (2017 *Lett.*)], the particle size is increased after annealing due to agglomeration of ZnO QDs [H. Kumar *et al*. (2017)]. The SEM image also shows some cracks between grain boundaries are created after annealing, which may help in the enhancement of gas

adsorption and hence the sensitivity of the sensor. The Atomic Force Microscopy (AFM, scanning probe microscopy, Model No. NTEGRA Prima, NT-MDT Services and Logistics Ltd., Ireland) of the annealed ZnO QDs deposited on SiO_2/Si substrate is shown in Figure 5.7. The peak-to-peak, root mean square (RMS) roughness, and average roughness values obtained from AFM analysis are 111.2, 14.2, and 11.2 nm, respectively. It is observed that the surface of deposited ZnO QDs is highly porous, which may help in increasing the gas adsorption and hence the sensitivity of the device.

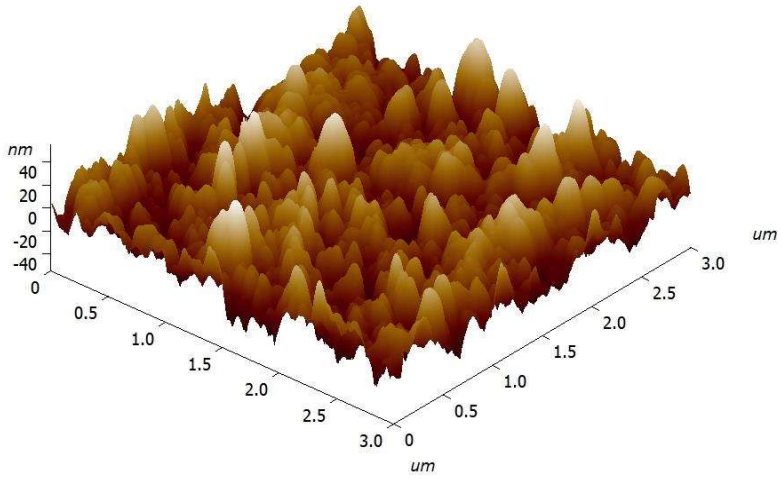

Figure 5.7: AFM image of the ZnO QDs thin film annealed at 450°C.

5.3.2 Electrical Characterization of MSM sensor

The electrical characteristic of the fabricated interdigitated MSM sensor is first measured in dark and ambient environmental conditions. This dark and ambient condition is achieved in the homemade gas sensing chamber having a water volume capacity of 10 liters with gas inlet and outlet valves, already discussed in Chapter 1. The specific amount of analyte gases in pure form without any balance/carrier gas are injected inside the gas chamber using an attached mass flow controller (MFC, model MC-100 SCCM from Alicat Scientific Inc., USA) at the inlet of the gas chamber. A heater is attached below the sample, holding a chuck at the bottom of the chamber to operate the sensor at various temperatures. The fabricated sensor is placed on the chuck

inside the chamber, and the interdigitated electrodes are connected to the semiconductor parameter analyzer (SPA, Model B1500A from Keysight) using a magnetic probe manipulator. The applied voltage is swept from -5 V to 5 V, and the corresponding current-voltage (*I-V*) curve is plotted in Figure 5.8 for different temperatures.

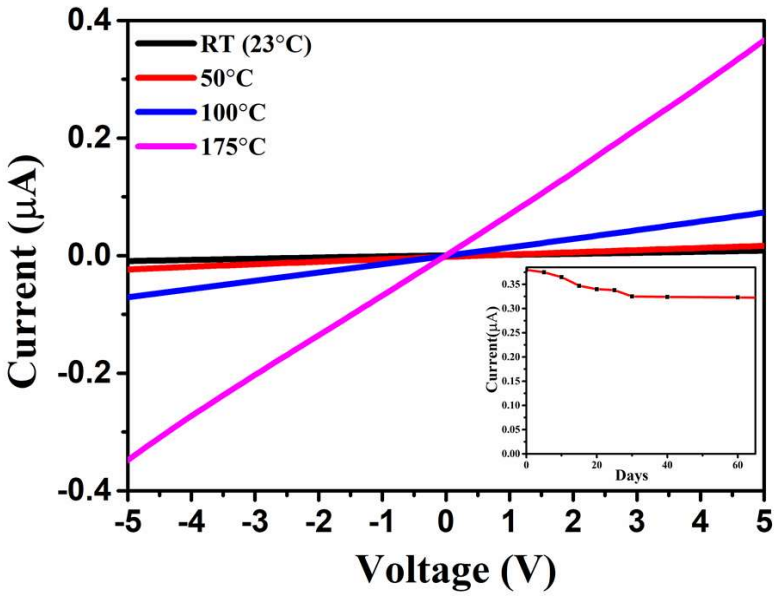

Figure 5.8: Current-voltage characteristic at different temperatures under unexposed conditions. The stability of the MSM sensor in an open-air atmosphere at 175°C and 5 V bias voltage in the inset.

The relative humidity (RH) in ambient air and room temperature condition was 56%. This RH value decreases with an increase in temperature. The values of RH were ~45, ~31 and ~15% at 50°C, 100°C, and 175°C, respectively. The *I-V* curve confirms the formation of nearly ohmic contact between ZnO QDs and Ag electrode. Over multiple measurement performance of the device was approximately identical in ambient condition. The fabricated MSM device is also characterized for long term stability in the open-air condition at 175°C temperature and 5 V bias voltage. The obtained investigation results are shown in the inset of Figure 5.8. It is found that the sensor

current in the ambient is relatively stable as compared to the sensor current obtained under H_2 gas exposure.

5.3.3 Gas sensing Characterization of MSM Sensor

The H_2 gas sensing characteristics are measured for different temperatures in an ambient air atmosphere at room temperature and increased temperature up to 175°C (corresponding change in relative humidity is ~56% to ~15%). The change in sensor current at different temperatures (23°C - 175°C) at 1% H_2 gas exposure to the sensor is shown in Figure 5.9.

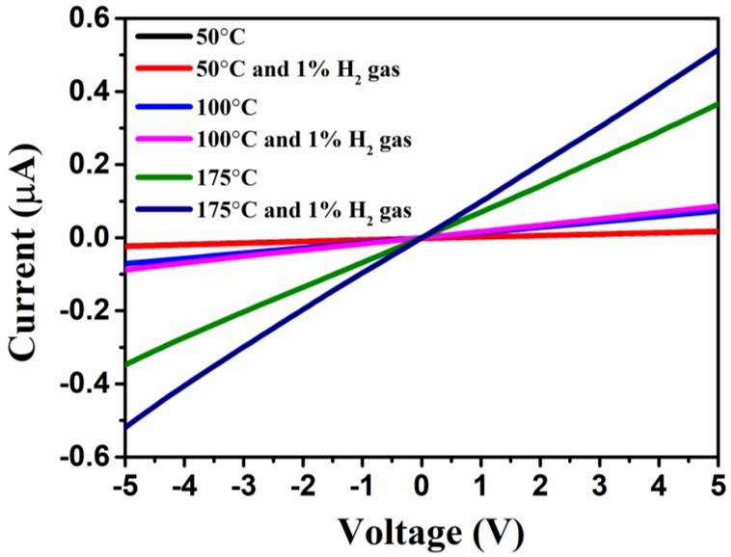

Figure 5.9: Current-voltage characteristic at different temperatures and exposure of 1% H_2 gas.

No significant H_2 gas response in the proposed ZnO QDs based MSM sensor is observed at room temperature (23°C). The H_2 gas response of the device is observed to be increased with temperature; similarly, more hydrogen atoms can reach the ZnO QDs surface, which reduces the channel resistance and hence increases the current at higher temperature [Rajan *et al*. (2016)]. Due to the maximum temperature limit of the sensing setup, the optimum sensing temperature is chosen at 175°C, and corresponding *IV* characteristics for different H_2 gas concentrations is shown in Figure 5.10. The increase in current with gas concentration is attributed to the decrease in channel resistance of

the proposed ZnO QDs based sensor.

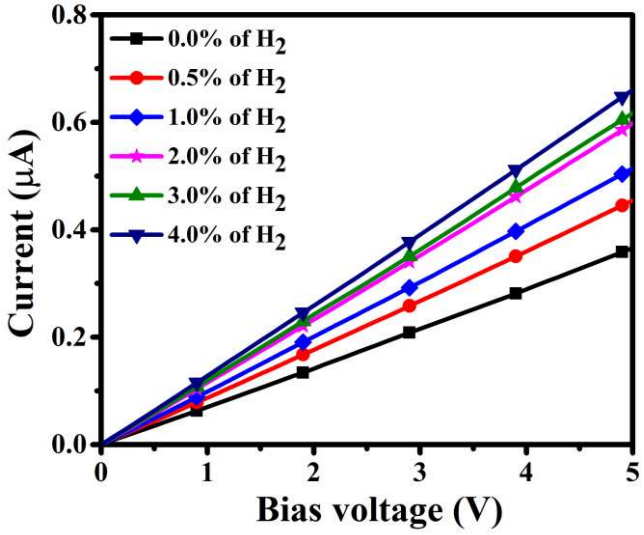

Figure 5.10: Current-voltage characteristic at different H_2 concentrations and fixed temperature of 175°C.

The gas sensing mechanism is basically a surface phenomenon that depends mainly on the activation energy of the target gas [Huh *et al.* (2011)]. It is the property of metal oxide that its electrical conductivity changes when several gases interact with its surface [Seiyama *et al.* (1962)]. On the surface of the semiconductor, the phenomena of adsorption and desorption appear very rapidly, which makes a significant change in the electrical conductivity of thin-film semiconductors, and this property of semiconductor thin films are used to detect the various gaseous components [Seiyama *et al.* (1962)]. The addition of a small amount of noble metal (e.g., Pt, Pd, Ag, Au, etc.) to metal oxide also increases the surface of the sensor with the analyte gases can be explained using oxidizing and reducing nature of gases [Das *et al.* (2010)]. At room temperature, ZnO surface adsorbs oxygen species from the air atmosphere and increases the film resistance. When the temperature of the sensor is increased, desorption of oxygen is started, which decreases the film resistance [Das *et al.* (2010)]. Here two type of adsorption occurs, first at room or lower temperature which decreases the conductivity and another at a higher or favorable temperature which increases the conductivity

[Yamazoe *et al.* (1979)]. Only some surface defects work as an adsorption site at a lower temperature, while at the higher temperature, some specific types of adsorption sites are available for adsorption, which increases the conductivity [Yamazoe *et al.* (1979)]. At room or lower temperature O_2^{-1} is the principal species of chemisorbed oxygen, whereas at the higher temperature, chemisorbed O_2^{-1} donates an electron to ZnO $(O_2^{-1} \rightarrow O_2 + e)$ [Chang. (1980)], hence conductivity increases already discussed in Chapter 1. When the proposed sensor is exposed to H_2 gas at higher temperatures, the H_2 molecules first react with the remaining adsorbed oxygen ion on the sensor surface and then with the ZnO surface [Das *et al.* (2010), Ren *et al.* (2011), Rajan *et al.* (2016)]. As a result, H_2 molecules create acceptor surface states, which release electrons to the conduction band of ZnO, which, in turn, decreases the film resistance and increases the current. The chemical reactions that occur at the surface are as follows [Ren *et al.* (2011)]:

$$\begin{aligned} 4H + O_2^- &\rightarrow 2H_2O + e^- \\ 2H + O^- &\rightarrow H_2O + e^- \\ 2H + O^{2-} &\rightarrow H_2O + 2e^- \end{aligned} \tag{5.1}$$

The gas response of the sensor is defined as the ratio of change in current under gas exposure to the original current in the air, which can be expressed as [Mondal *et al.* (2014)]

$$Gas\ response(S) = \frac{I_{H_2} - I_{air}}{I_{air}} \times 100\% \tag{5.2}$$

where, I_{air} and I_{H2} are the currents measured under ambient air and different H_2 concentrations, respectively. The gas response of the proposed ZnO QDs based H_2 sensor is shown in Figure 5.11 for different H_2 concentrations and different applied bias voltage at 175°C. It is observed from the results that the effect of bias voltage on the gas

response of the proposed device is nearly negligible. The slope of this gas response curve is defined as the sensitivity of the sensor expressed in ppm^{-1} [Giancaterini *et al.* (2015)].

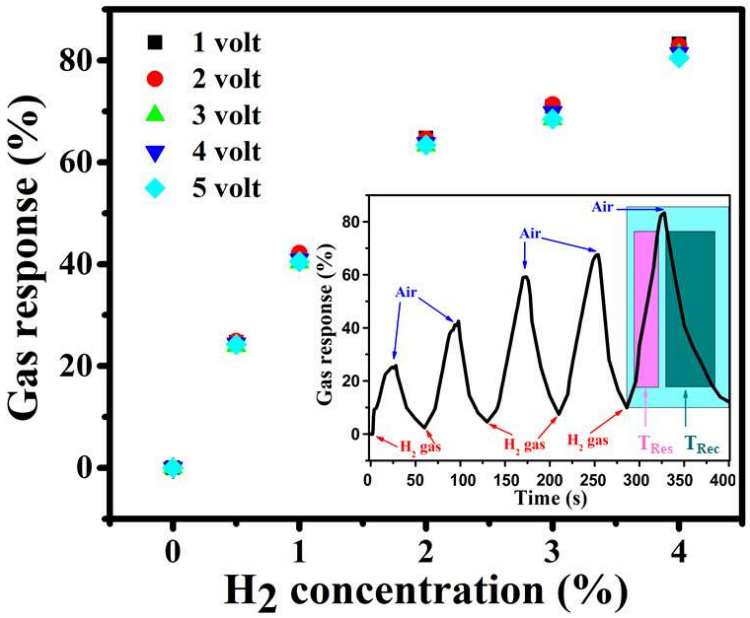

Figure 5.11: Gas response - H_2 concentration plot at different bias voltage and temperature of 175°C. Inset shows the response-recovery characteristics for H_2 gas at an applied bias of 1 V.

The gas response is increased with the H_2 concentration, but the response to be saturated at a higher concentration of H_2. The gas responses are 24.6%, 41.1%, and 83.2% for 0.5% H_2, 1% H_2, and 4% H_2 gas, respectively. It may be mentioned that the gas response of any thin-film sensor increases with the decrease in grain size below 10 nm [Malagu *et al.* (2002)]. In this work, the synthesized ZnO QDs have an average particle size of ~2.53 nm, which results in the enhanced gas response of as high as 83.2% for 4% of H_2 concentration at 175°C. The response and recovery characteristics are performed for the determination of response time (T_{Res}, time taken from 10% to 90% response) and recovery time (T_{Rec}, time is taken from 90% to 10% response) for H_2 gas as shown in the inset of Figure 5.11. The values of T_{Res} and T_{Rec} are calculated as ~27 s and ~56 s, respectively under exposure of 4% H_2 gas. In this case we also fabricate the set of 10 device and sensors made using ZnO QDs have shown high

stability and repeatability in the ambient environment and identical conditions. The percentage deviation in the responses were ±2%.

The selectivity of the H_2 sensing with respect to ammonia, sulfur dioxide, and organic vapors such as acetone, methanol, chlorobenzene, and chloroform is shown in Figure 5.12 with corresponding error of ~2%.

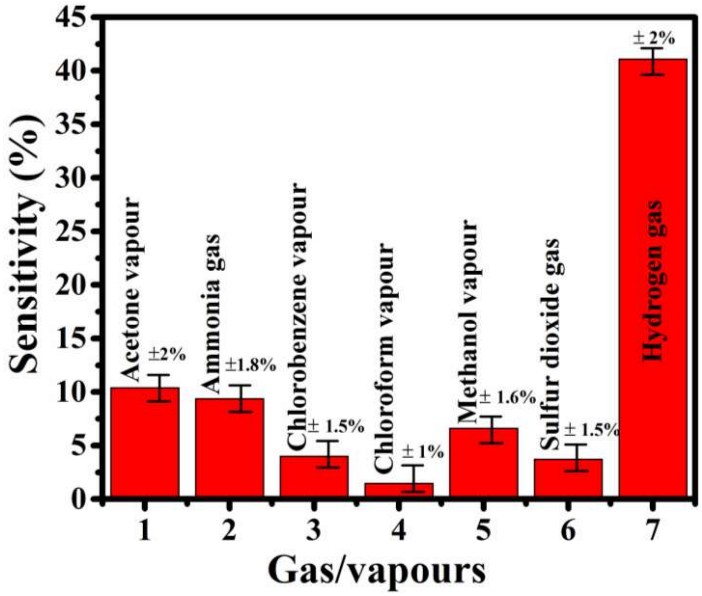

Figure 5.12: Gas response of the hydrogen gas sensor over common interference gases and organic vapors at a temperature of 175°C.

The selectivity of the proposed sensor is measured for 1% concentrations of the interfering gases and vapors mentioned above. Note that the sensitivities of the proposed sensor for 1% of each of ammonia gas, sulfur dioxide gas, acetone, chlorobenzene, chloroform, and methanol are 9.3% and 3.7%, 10.4%, 4.0%, 1.5%, and 6.6%, respectively at 175°C which are very small as compared to the sensitivity of 41.1% corresponding to the H_2 gas. For the environmental effect, we have investigated the selectivity of the sensors in the presence of various interference species generally found along with hydrogen gas. It is obvious from the selectivity characteristics that the hydrogen responses are less affected by the interference species present in the harsh environment.

5.4 Conclusion

In this chapter, the electrical and gas sensing characteristics of colloidal ZnO QDs thin-film based interdigitated MSM sensor for H_2 gas sensing have been investigated. The ZnO QDs synthesized by the hot injection method is deposited on the Si/SiO_2 substrate by spin coating technique. The XRD and EDS are used to confirm the presence of ZnO QDs, whereas SEM and AFM analyses are used to analyze the surface morphology of the ZnO QDs thin film. The proposed MSM sensor shows a negligible hydrogen sensitivity at room temperature but the maximum sensitivity of 83.2% at 4% hydrogen at 175°C. The proposed ZnO QDs based MSM sensor also shows a very good H_2 selectivity with respect to other interference gases, namely ammonia, sulfur dioxide, and various organic vapors such as acetone, chlorobenzene, chloroform, and methanol. However, the hydrogen sensitivity of the proposed sensor is found to be nearly independent of the applied bias voltage.